Chapter 11

Thermoelectric Refrigeration Principles

Diana Enescu

Additional information is available at the end of the chapter

http://dx.doi.org/10.5772/intechopen.75439

Abstract

This chapter recalls the general principles and main formulations useful in the study of thermoelectric coolers. Starting from the general heat diffusion equation, analytical expressions are introduced for the determination of cooling capacity and rate of heat rejection in steady-state conditions. When dealing with the whole refrigeration system, the limits of the steady-state analysis of the individual thermoelectric elements are pointed out, indicating the need for transient analysis supported by experimental evaluations. Then, the energy indicators are illustrated by considering the electrical power consumption, the thermal performance described by the dimensionless figure of merit, as well as the coefficient of performance. Furthermore, the main methods to enhance the thermoelectric cooler performance in refrigeration units are highlighted, with reference to high-performance materials, design aspects and temperature control systems. Finally, indications are reported on some applications of various thermoelectric refrigeration solutions, considering the technical aspects of the performance of these systems.

Keywords: refrigeration, thermoelectric unit, energy indicators, cooling capacity, coefficient of performance, temperature control, renewable sources

1. Introduction

The thermoelectric effect represents direct conversion of the temperature difference into voltage and vice versa and refers to phenomena with which the current flows through the thermoelements or legs of a thermoelectric module. The thermoelectric effect is formed due to free motion of the charge carriers (free electrons e^- considered as negative charge carriers and holes h^+ considered as positive charge carriers) in metals and semiconductors while carrying energy and electric charge. In this case, the electric effects are accompanied by thermal effects and vice versa [1]. The thermoelectric effects are Peltier effect, Thomson effect and Seebeck effect. The *Peltier effect* is the phenomenon that converts current to temperature and occurs when an

electric current flows through a thermoelectric device. The Peltier effect is a reversible phenomenon, because the Peltier heat depends directly on the direction of the carrier flow or electrical current [2].

There is interdependence between the sense of the electric current and the temperature difference at the hot and cold ends of a thermoelectric device. In other words, if the current flow is changed, the temperature at the hot and cold ends is changed as well.

The heat flow rate is given by

$$\dot{Q}_{\text{Peltier}} = \pi_{\text{AB}} \cdot I \cdot T = (\pi_{\text{B}} - \pi_{\text{A}}) \cdot I \cdot T \tag{1}$$

where $\dot{Q}_{\text{Peltier}}$ is the absorbed or dissipated heat flow rate, in W; I is the electric current that flows through the junctions, in A; π_{AB}, π_{A} and π_{B} are the Peltier coefficients of the thermocouple and conductors A and B, in $\text{W}\cdot\text{A}^{-1}$; and T is the absolute temperature, in K.

The Peltier coefficient π is defined as the amount of heat developed or absorbed at a junction of a thermocouple when a current of one ampere passes through this junction for one second. The Peltier coefficient π is positive for heat absorbed and negative for heat dissipated. The Peltier coefficient determines a cooling effect when the current flows from the N-type semiconductor material to a P-type semiconductor material and a heating effect when the current flows from the P-type semiconductor material to an N-type semiconductor material.

The *Thomson effect* is given by generation or absorption of a heat quantity in a homogeneous conductor by which an electric current flows and where there is a temperature gradient. The heat absorbed or released depends on the electric current direction and the conductor material. The *Thomson effect* is a reversible thermoelectric phenomenon and is observed when the charge carriers change energy levels.

The convention for the Thomson effect is:

- *positive* Thomson effect, when the hot end has a high voltage and the cold end has a low voltage; the heat is generated when the current flows from the hotter junction to the colder junction, while the heat is absorbed when the current flows from the colder end to the hotter end.
- *negative* Thomson effect, when the hot end has a low voltage and the cold end has a high voltage; the heat is generated when the current flows from the colder junction to the hotter junction, while the heat is absorbed when the current flows from the hotter end to the colder end; some metals have negative Thomson coefficients (e.g. Co, Bi, Fe, and Hg) [3].

The Thomson heat flow rate $\dot{Q}_{\text{Thomson}}$ is proportional to the thermal gradient as well as to the intensity of the electric current which flows through the conductor:

$$\dot{Q}_{\text{Thomson}} = -\mu_{\text{AB}} \cdot I \cdot \nabla T = (\mu_{\text{B}} - \mu_{\text{A}}) \cdot I \cdot \nabla T \tag{2}$$

where μ_{AB} is the Thomson coefficient in $\text{V}\cdot\text{K}^{-1}$, I is the electric current flowing through the circuit supplied by a voltage and $\nabla T = \frac{\text{d}T}{\text{d}x}$ is the temperature gradient along the conductor.

http://dx.doi.org/10.5772/intechopen.75439

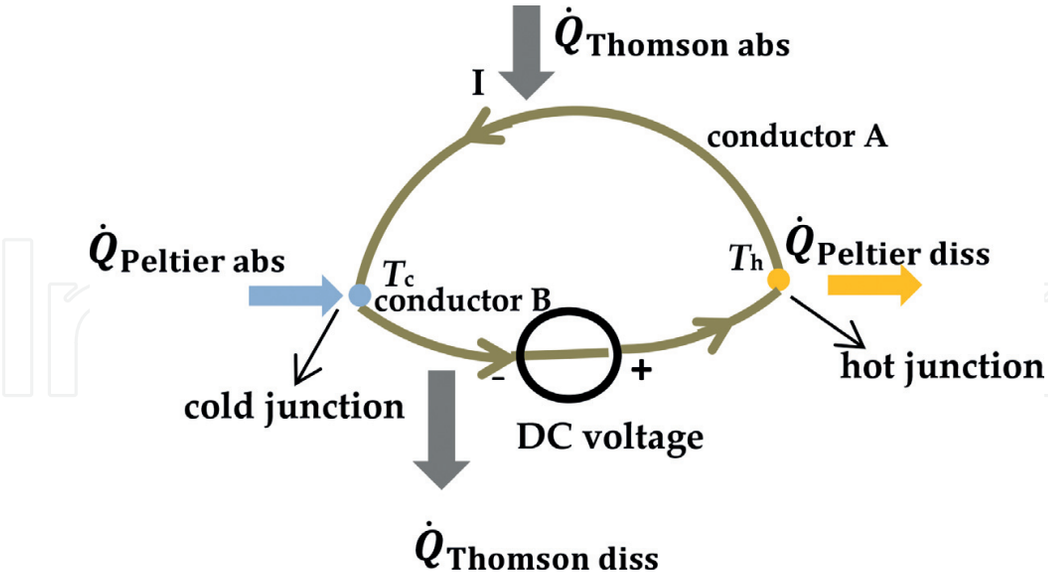

Figure 1. Schematic of Peltier effect and Thomson effect in a thermocouple.

With reference to **Figure 1**, the sign convention of the Thomson coefficient is positive for heat absorbed (conductor A) and negative for heat dissipated (conductor B).

Furthermore, the *Joule* heat $\dot{Q}_{\text{Joule}}$, in W, is irreversible and takes place in a conductor with electrical current flow, regardless of the direction of the current. Its expression is given by

$$\dot{Q}_{\text{Joule}} = R \cdot I^2 \tag{3}$$

where R is the conductor resistance in Ω.

If a current density J exists through a homogeneous conductor, the heat production per unit volume or volumetric heat generation is

$$\dot{q}_{\text{v}} = \underbrace{\rho \cdot J^2}_{\text{Joule heating}} \underbrace{- \mu \cdot J \cdot \nabla T}_{\dot{Q}_{\text{Thomson}}} = \rho \cdot \left(\frac{I}{S}\right)^2 - \mu \cdot \frac{I}{S} \cdot \nabla T \tag{4}$$

where ρ is the electrical resistivity of the material in Ω·m, $J = \frac{I}{S}$ is the current density in $\text{A} \cdot \text{m}^{-2}$ and S is the cross-sectional area in m^2.

The *Seebeck effect* converts temperature to current and occurs like the Peltier effect, but the direction of the electric current is reversed. The Seebeck effect appears when a temperature gradient along a conductor provides a voltage increment. In other words, the Seebeck voltage drives the hole/electron flow due to a temperature difference which does exist in the conductor between the high- and low-temperature regions. The Seebeck voltage appearing at the circuit junctions is

$$\Delta V = \alpha_{\text{AB}} \cdot \Delta T = (\alpha_{\text{A}} - \alpha_{\text{B}}) \cdot (T_{\text{H}} - T_{\text{C}}) \tag{5}$$

where α_A, α_{B} are the Seebeck coefficients for the conductors A and B, in $\text{V} \cdot \text{K}^{-1}$.

The Seebeck coefficient or thermoelectric power is a very important parameter for the thermoelectric materials, determining the *performance of Peltier elements*. For a good thermoelectric material, the Seebeck coefficient has to be high in order to obtain the desired voltage more easily, the electrical conductivity has to be high, and the thermal conductivity has to be small to reduce the thermal losses in the junctions of the thermocouple [4].

The relationship of the Seebeck coefficient to the electric field E and the temperature gradient ∇T is

$$\alpha_{AB} = \frac{E}{\nabla T} \tag{6}$$

The sign of the Seebeck coefficient depends on the hole and electron flow:

- A negative Seebeck coefficient is obtained in semiconductors negatively doped (e.g. N-type semiconductors).
- A positive Seebeck coefficient is obtained in semiconductors positively doped (e.g. P-type semiconductors).

There is interdependence between the Peltier coefficient and the Seebeck coefficient, as well as between the Seebeck coefficient and the Thomson coefficient, given by the following relationships [5, 6]:

$$\pi_{AB} = \alpha_{AB} \cdot T \tag{7}$$

$$\mu_{AB} = T \cdot \frac{d\alpha_{AB}}{dT} \tag{8}$$

A thermoelectric cooler (TEC) is a semiconductor composed of an electronic component which transforms electrical energy into a temperature gradient. The TEC consists of one or more thermoelectric couples. A thermoelectric couple is a couple having one P-type thermoelectric leg (an excess of holes h^+, positive Seebeck coefficient α_P, electrical resistivity ρ_P and thermal conductivity k_N) and one N-type thermoelectric leg (an excess of free electrons e^-, negative Seebeck coefficient α_N, electrical resistivity ρ_N and thermal conductivity k_N linked to each other by an electrical conductor (a conductive metallic strip) forming a junction. The thermoelectric couples are connected in such a way that when the current flows through the device, both the P-type holes and the N-type electrons move towards the same side of the device.

The two legs are made of two different thermoelectric materials. A thermoelectric material is defined as an alloy of materials that generates thermoelectric properties (thermal conductivity, electric conductivity and Seebeck coefficient). The quality as a semiconductor material to be cooled strictly depends on the transport properties of the material (Seebeck voltage, electrical resistivity and thermal conductivity) as well as the operational temperature field between the cold and hot ends [5]. Considering that the input voltage of a single thermoelectric couple is reduced, many thermoelectric couples are connected to

each other by junctions and are sandwiched between two ceramic substrates to form a thermoelectric module (TEM). These ceramic substrates act as insulator from electrical point of view but allow the thermoelectric couples to be thermally in parallel. The number of thermoelectric couples is influenced by the needed cooling capacity and the maximum electric current [5]. When a low voltage DC power source is applied to the free end of the TEM, the heat flow rate is transferred from one side to other side of the device through the N- and P-semiconductor legs and junctions. In this case, one side of the TEM is cooled, and the other side is heated [7]. In the cooling mode, the sense of the electrical current is from the N-type semiconductor to the P-type semiconductor (**Figure 2**). The Seebeck voltage is generated in the device when there is a temperature difference between the junctions of the thermoelements [8].

The direction of the current is then essential to establish the functionality of the device. If the direction of the electrical current is reversed, the compartment would be heated instead of being cooled.

At the top of every junction, the temperature is the same (T_c), and at the bottom of every junction, the temperature is the same (T_h). At the cold junction, the temperature T_c decreases, and the heat $\dot{Q}_c$ is absorbed from the compartment which must be cooled. Through the cold junction, the electrons are transported from a low energy level inside the P-type semiconductor legs to a high energy level inside the N-type semiconductor legs. At the hot junction, the heat $\dot{Q}_h$ is transferred according to the transport electrons. This heat is dissipated at the heat sink (a passive heat exchanger that cools a device by dissipating heat into the environment), and the free electrons flow to an inferior energy level in the P-type semiconductor.

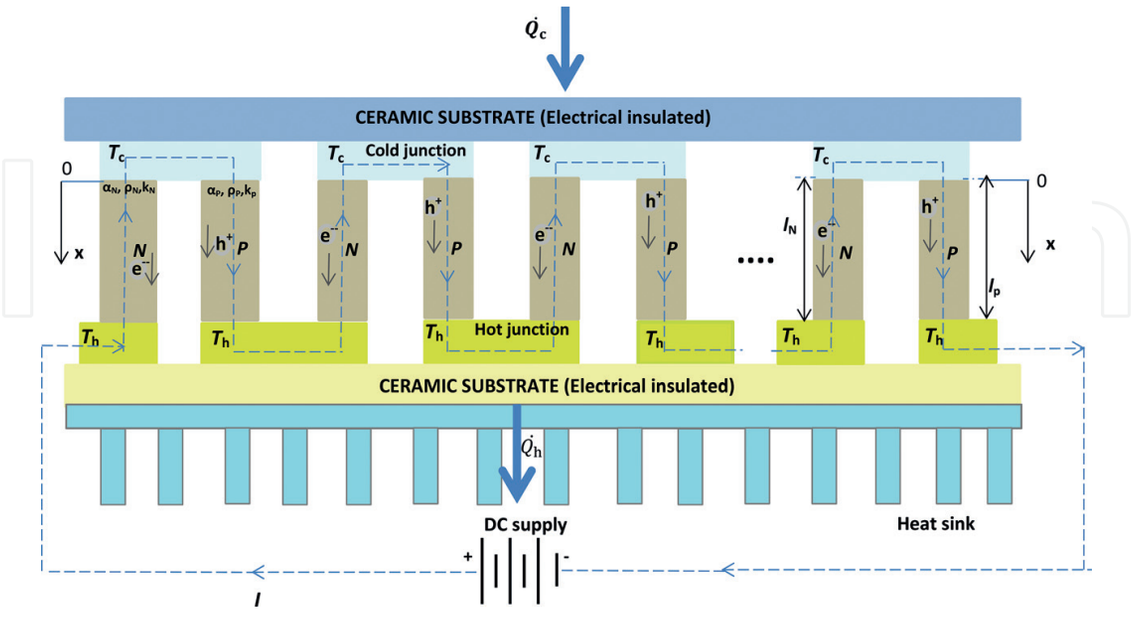

Figure 2. Schematic of a thermoelectric module (TEM) operating in cooling mode.

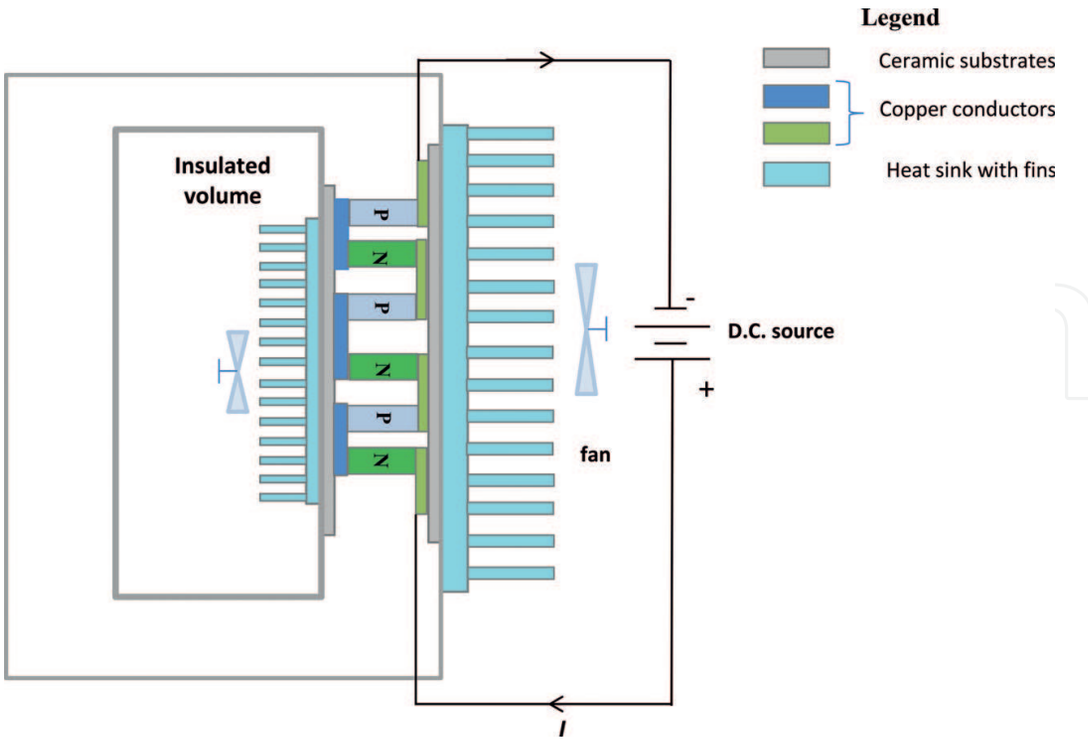

Figure 3. Schematic of a TEM used for the refrigeration unit.

The main components of a refrigeration unit (**Figure 3**) are [7, 9, 10]:

- the insulated refrigerator *cabinet* with thermoelectric technology having variable dimensions (e.g. for a capacity from 5 to 40 l, the thickness is from 5 to 10 cm, and for a capacity less than 5 l the thickness is 4 cm);
- the cooling thermoelectric system with semiconductors (TECs) useful to cool the insulated volume;
- the *heat sink*, considered as a heat exchanger useful to facilitate the heat transfer from the hot side of TEC to the environment. The TEC can operate in a definite operating range of its temperature difference. To keep this temperature difference inside the specific operating range, a TEC is compulsory to have a heat sink at the hot end to dissipate heat from the TEC to environment. Sometimes, another heat sink with fins is fixed inside the compartment to improve the heat transfer from the insulated volume which is cooled (fluid, solid) to the cold side of the TEC. In this case, the heat sink is cooled at a temperature lower than the insulated volume, and the heat flowing between the fins is collected by means of a fan [11–13];
- one or many *fans* which transfer heat through convection and allow the dissipation of heated or cooled air in order to avoid operational problems; the fans are powered by the same external power supply that powers the TEC;
- the control system useful for an accurate temperature control; as the current value is changing, it is possible to directly control the cooling capacity.

http://dx.doi.org/10.5772/intechopen.75439

2. Theoretical assessment of a thermoelectric cooler

2.1. The general heat diffusion equation

Consider a non-uniformly heated thermoelectric material having isotropic properties (the same transport properties in all directions) crossed by a constant current density $\vec{J}$ [2, 14–16]. The continuity equation is

$$\vec{\nabla} \cdot \vec{\mathrm{J}} = 0 \tag{9}$$

where $\vec{J}$ is the current density vector and $\vec{\nabla}$ is the gradient vector, a differential operator with respect to the three orthogonal directions:

$$\vec{\nabla} = \vec{i}\,\frac{\partial}{\partial x} + \vec{j}\,\frac{\partial}{\partial y} + \vec{k}\,\frac{\partial}{\partial z} \tag{10}$$

A temperature gradient generates an electric field $\vec{E}$. This electric field depends on the temperature gradient $\vec{\nabla} T$ and on the current density $\vec{J}$ and is expressed as

$$\vec{E} = \underbrace{\rho \cdot \vec{J}}_{\text{Ohm's law}} + \underbrace{\alpha \cdot \vec{\nabla} T}_{\textit{Seebeck voltage}} \tag{11}$$

with the electrical resistivity ρ in Ω·m and the Seebeck coefficient α in $\mathrm{V \cdot K^{-1}}$.

The heat flow rate $\vec{q}$ also depends on the temperature gradient $\vec{\nabla} T$ and is expressed as

$$\vec{q} = \underbrace{-k \cdot \vec{\nabla} T}_{\text{Fourier's law}} + \underbrace{\alpha \cdot T \cdot \vec{J}}_{\text{Peltier heat}} \tag{12}$$

where k is the thermal conductivity in $\mathrm{W \cdot (m \cdot K)^{-1}}$.

The general heat diffusion equation for transient state [14] is

$$-\vec{\nabla} \cdot \vec{q} + \dot{\mathrm{q}}_{\mathrm{vol}} = \rho \cdot c_{\mathrm{p}} \cdot \frac{\partial T}{\partial t} \tag{13}$$

where ρ is the electrical resistivity in Ω·m, c_{p} is the specific heat capacity at constant pressure in $\mathrm{J \cdot (kg \cdot K)^{-1}}$ and $\dot{q}_{\mathrm{vol}}$ is the volumetric heat generation, in $\mathrm{W \cdot m^{-3}}$.

The volumetric heat generation is also given by

$$\dot{\mathrm{q}}_{\mathrm{vol}} = \vec{E} \cdot \vec{J} = \left(\rho \cdot \vec{J} + \alpha \cdot \vec{\nabla} T\right) \cdot \vec{J} = \rho \cdot \mathrm{J}^2 + \vec{J} \cdot \alpha \cdot \vec{\nabla} T \tag{14}$$

Based on Thomson's relationship and Osanger's relationship, the heat flow rate vector is written as [16]

$$\vec{q} = \alpha \cdot T \cdot \vec{J} - k \cdot \vec{\nabla} T \tag{15}$$

Substituting Eq. (14) and Eq. (15) into Eq. (13), with successive elaborations, yields

$$\rho \cdot \mathrm{J}^2 + \vec{J} \cdot \alpha \cdot \vec{\nabla} T = \vec{\nabla} \cdot \vec{q} + \rho \cdot c_\mathrm{p} \cdot \frac{\partial T}{\partial t}$$

$$\rho \cdot \mathrm{J}^2 + \vec{J} \cdot \alpha \cdot \vec{\nabla} T = \vec{\nabla} \cdot \left(-k \cdot \vec{\nabla} T + \alpha \cdot T \cdot \vec{J} \right) + \rho \cdot c_\mathrm{p} \cdot \frac{\partial T}{\partial t}$$

$$\rho \cdot \mathrm{J}^2 + \vec{J} \cdot \alpha \cdot \vec{\nabla} T = -\vec{\nabla} \cdot \left(k \cdot \vec{\nabla} T \right) + \underbrace{\vec{\nabla} \cdot \left(\alpha \cdot T \cdot \vec{J} \right)}_{T \cdot \vec{J} \cdot \frac{\mathrm{d}\alpha}{\mathrm{d}T} \vec{\nabla} T + \vec{J} \cdot \alpha \cdot \vec{\nabla} T} + \rho \cdot c_\mathrm{p} \cdot \frac{\partial T}{\partial t} \tag{16}$$

Considering that $\mu = T \cdot \frac{\mathrm{d}\alpha}{\mathrm{d}T}$ is the Thomson coefficient, the heat diffusion equation is

$$\underbrace{\vec{\nabla} \cdot \left(k \cdot \vec{\nabla} T \right)}_{\textit{thermal conduction}} + \underbrace{\rho \cdot \mathrm{J}^2}_{\textit{Joule heating}} - \underbrace{\mu \cdot \vec{J} \cdot \vec{\nabla} T}_{\textit{Thomson effect}} = \underbrace{\rho \cdot c_\mathrm{p} \cdot \frac{\partial T}{\partial t}}_{\text{transient}} \tag{17}$$

2.2. Steady-state and transient approaches

2.2.1. The limits of steady-state analysis

Steady-state analysis for a TEC is typically carried out by resorting to a set of approximations. The simplest model is based on the following assumptions: the Seebeck effect does not depend on temperature, there are no thermal or electrical contact resistances, there are no heat losses, and the Thomson coefficient is zero ($\mu = 0$), so that the Thomson heat is absent [2, 14, 16]. In these conditions, there is no heat transfer from or to the external environment, so that the heat flows occur only between the source and the sink. On these assumptions, Eq. (17) becomes

$$\vec{\nabla} \cdot \left(k \cdot \vec{\nabla} T \right) + \rho \cdot \mathrm{J}^2 = 0 \tag{18}$$

By replacing in Eq. (18) the current density $J = \frac{I}{S}$ and the temperature Laplacian $\nabla^2 T = \vec{\nabla} \cdot \vec{\nabla} T = \vec{i} \frac{\partial}{\partial x} \cdot \vec{i} \frac{\partial T}{\partial x} = \frac{\mathrm{d}^2 T}{\mathrm{d}x^2}$, the one-dimensional differential equation is [2, 14–16]

$$k \cdot S \cdot \frac{\mathrm{d}^2 T}{\mathrm{d}x^2} + \rho \cdot \frac{I^2}{S} = 0 \Rightarrow k \cdot S \cdot \mathrm{d}\left(\frac{\mathrm{d}T}{\mathrm{d}x} \right) = -\rho \cdot \frac{I^2}{S} \mathrm{d}x \tag{19}$$

Let us consider the boundary conditions between the following limits (**Figure 4**):

$$x = 0 \Rightarrow T = T_c \tag{20}$$

$$x = l \Rightarrow T = T_h \tag{21}$$

The heat flow rate at $x = 0$ and $T = T_\mathrm{c}$ is expressed as

$$\dot{Q}_{x=0} = \alpha \cdot I \cdot T_\mathrm{c} - k \cdot S \left. \frac{dT}{dx} \right|_{x=0} \Rightarrow \dot{Q}_{x=0} = \alpha \cdot I \cdot T_\mathrm{c} - \frac{\rho \cdot I^2}{2S} \cdot l - (T_\mathrm{h} - T_\mathrm{c}) \cdot \frac{k \cdot S}{l} \tag{22}$$

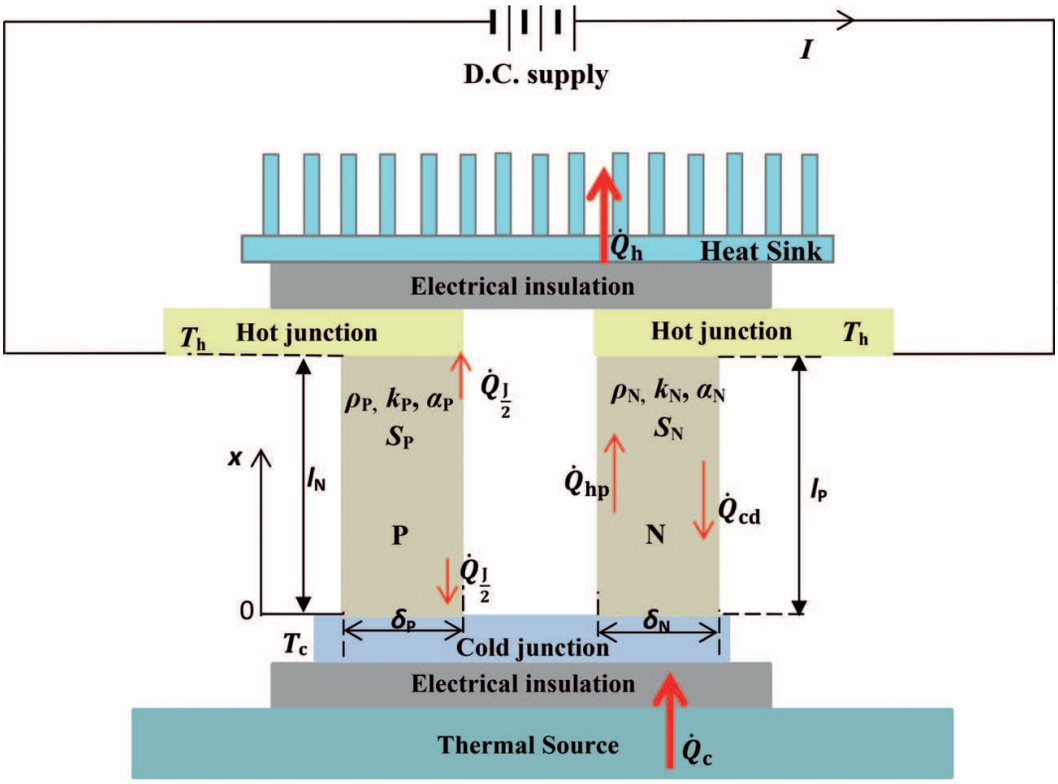

Figure 4. Schematic of a TEC (geometric elements and material properties).

and the heat flow rate at $x = l$ and $T = T_h$ is

$$\dot{Q}_{x=l} = \alpha \cdot I \cdot T_h - k \cdot S \left.\frac{dT}{dx}\right|_{x=l} \Rightarrow \dot{Q}_{x=l} = \alpha \cdot I \cdot T_h + \frac{\rho \cdot I^2}{2S} \cdot l - (T_h - T_c) \cdot \frac{k \cdot S}{l} \tag{23}$$

The heat flow rate at the cold junction is obtained by summing up the contributions of the N-type and P-type elements at $x = 0$:

$$\dot{Q}_c = \dot{Q}_{x=0,\,P} + \dot{Q}_{x=0,\,N} \tag{24}$$

$$\dot{Q}_c = (\alpha_P - \alpha_N) \cdot I \cdot T_c - \frac{1}{2} \cdot \left(\frac{\rho_P \cdot l_P}{S} + \frac{\rho_N \cdot l_N}{S} \right) \cdot I^2 - \left(\frac{k_P \cdot S_P}{l_P} + \frac{k_N \cdot S_N}{l_N} \right) \cdot (T_c - T_h) \tag{25}$$

Likewise, the heat flow rate at the hot junction is determined for $x = l$:

$$\dot{Q}_h = \dot{Q}_{x=l,\,P} + \dot{Q}_{x=l,\,N} \tag{26}$$

$$\dot{Q}_h = (\alpha_P - \alpha_N) \cdot I \cdot T_h + \frac{1}{2} \cdot \left(\frac{\rho_P \cdot l_P}{S} + \frac{\rho_N \cdot l_N}{S} \right) \cdot I^2 - \left(\frac{k_P \cdot S_P}{l_P} + \frac{k_N \cdot S_N}{l_N} \right) \cdot (T_h - T_c) \tag{27}$$

The total electrical resistance R of the thermoelement pair in series, the total thermal conductance K of the thermoelements in parallel, the Seebeck coefficient α_{NP} of the thermoelectric

couple and the temperature difference ΔT between the hot surface temperature T_h and the cold surface temperature T_c are written as [9]

$$R = \frac{\rho_P \cdot l_P}{S} + \frac{\rho_N \cdot l_N}{S} \tag{28}$$

$$K = \frac{k_P \cdot S_P}{l_P} + \frac{k_N \cdot S_N}{l_N} \tag{29}$$

$$\alpha_{NP} = \alpha_P - \alpha_N \tag{30}$$

$$\Delta T = T_h - T_c \tag{31}$$

Considering that N-type and P-type thermocouples are identical (with the same length), the total electrical resistance is $R = \rho \cdot l \cdot (S)^{-1}$ with $\rho = \rho_P + \rho_N$, the total thermal conductance of the thermoelements is $K = k \cdot S \cdot (l)^{-1}$ with $k = k_P + k_N$ the thermal conductivity corresponding to the N and P thermoelement legs in $W \cdot (m \cdot K)^{-1}$, and σ is the electrical conductivity corresponding to the N and P thermoelement legs with $\sigma = \sigma_P + \sigma_N$ in $S \cdot m^{-1}$. Then, Eq. (24) and Eq. (26) give the cooling capacity (or the rate of heat absorbed at the cold junction) $\dot{Q}_c$ and the rate of heat rejection $\dot{Q}_h$ in W:

$$\dot{Q}_c = \alpha_{NP} \cdot I \cdot T_c - \frac{1}{2} \cdot R \cdot I^2 - K \cdot \Delta T \Rightarrow \dot{Q}_c = \dot{Q}_{hp} - \frac{1}{2}\dot{Q}_J - \dot{Q}_{cd} \tag{32}$$

$$\dot{Q}_h = \alpha_{NP} \cdot I \cdot T_h + \frac{1}{2} \cdot R \cdot I^2 - K \cdot \Delta T \Rightarrow \dot{Q}_h = \dot{Q}_{hp} + \frac{1}{2}\dot{Q}_J - \dot{Q}_{cd} \tag{33}$$

where $\dot{Q}_{hp}$ is the thermoelectric heat pumping at the cold junction, $\dot{Q}_J$ is the Joule heat and $\dot{Q}_{cd}$ is the heat flow conducted from the hot junction to the cold junction.

However, this model can be used only at first approximation for the selection of thermocouple materials [9]. In practice, the semiconductor properties depend on temperature, the contact resistances cannot be avoided, and the Thomson effect cannot be neglected. Moreover, in the steady-state model, the temperatures T_h and T_c are input values that have to be determined accurately. If the object to be cooled is directly in contact with the TEC cold surface, the object temperature has the same value as the temperature of the TEC cold surface T_c. However, if the object to be cooled is not directly in contact with the TEC cold surface, e.g. in a refrigerator compartment, a heat exchanger is required on the TEC cold surface. In this case, the cold surface of the TEC has to be some degrees colder than the desired temperature in the refrigerator compartment, and the temperature T_c is unknown. With a similar reasoning, if a heat exchanger is placed at the hot side, the known value is the ambient temperature, and the temperature T_h is unknown. The temperature distribution of a complex system (refrigerator) with TEC is depicted in **Figure 5**.

Therefore, in practical applications in which the TEC is connected to other components (e.g. heat exchangers), (i) the temperatures T_c and T_h are unknown, (ii) only the external temperatures can be measured accurately, and (iii) the temperature at each point of the system depends

http://dx.doi.org/10.5772/intechopen.75439

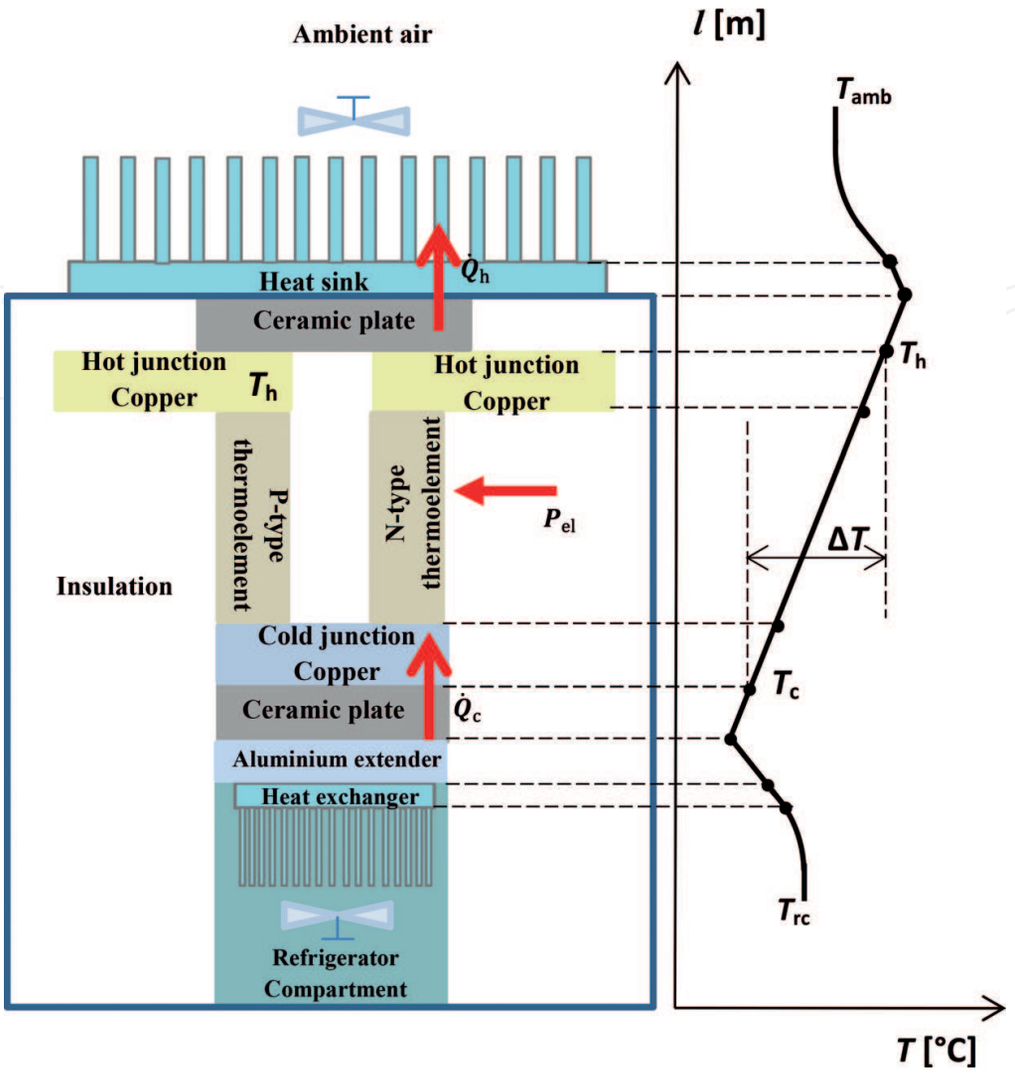

Figure 5. Schematic of temperature profile in a thermoelectric refrigeration system.

on the composition of the whole system and cannot be determined for the individual components. Thereby, the temperatures at the TEC terminals can be determined by using a dedicated model of the interconnected components. These temperatures are calculated from the solution of the overall system equations, in which all the temperature-dependent thermoelectric effects (Peltier, Seebeck, Thomson and Joule) are taken into account [17].

2.2.2. Transient analysis

Thermoelectric refrigerators are controlled devices that operate in transient conditions. Thereby, it is important to formulate a detailed model taking into account all the thermoelectric effects and the dependence of the model parameters on temperature.

Eq. (17) is written in generic transient conditions. The solution of this equation has been obtained in [18] by constructing an electrothermal equivalent model with resistances and capacities (in which the thermoelectric modules are represented through a multi-node structure and the other

components are represented by a single node). The implicit finite difference method has been used to solve the equations. In this model, the input data are the number of modules, the geometric parameters (lengths and cross areas), the structural characteristics of the components, the heat flow rate produced by the heat source, the voltage supply from the electrical system and the environment temperature. The structural characteristics can be given as constant values (density, specific heat, surface electrical resistivity of the thermoelectric elements) or can be expressed as functions of the temperatures (Seebeck coefficient, electrical resistivity and thermal conductivity). Since the model is non-linear, the solution requires an iterative process, so that the initialization of the temperatures at each node of the model has to be provided as well. The outputs of the method (with their evolutions in time) are the temperatures at all the nodes, the heat flow rates in each component, the power produced by the modules and consumed by the fan and the efficiencies of the modules and of the system. This formulation is consistent with an experimental application, such as the one presented in [17].

2.3. Energy indicators for TEC performance

The energy indicators useful for the design and the performance of TEC are the cooling capacity, the rate of heat rejection, the input electrical power, the dimensionless figure of merit ZT and the coefficient of performance (COP).

The temperature difference ΔT created when a current flows through the TEC generates a raising voltage [9]. This voltage depends on the voltage referring to the Seebeck effect $\alpha_{\mathrm{NP}} \cdot \Delta T$ and the voltage at the thermoelectric couple $\alpha_{\mathrm{NP}} \cdot \Delta T$:

$$V = \alpha_{\mathrm{NP}} \cdot \Delta T + R \cdot I \tag{34}$$

The input electrical power $\mathrm{P_{el}}$ or electrical power consumption [19] is

$$P_{\mathrm{el}} = \dot{Q}_h - \dot{Q}_c = \alpha_{NP} \cdot I \cdot \Delta T + R \cdot I^2 \tag{35}$$

An important physical property of the TEM is the figure of merit Z. It depends on the transport parameters (Seebeck coefficient of the thermoelectric couple, total electrical resistivity and total thermal conductivity):

$$Z = \frac{\alpha_{\mathrm{NP}}^2}{\rho \cdot k} \tag{36}$$

The thermal performance of a thermoelectric cooler is given by dimensionless figure of merit ZT. The absolute temperature T is the mean device temperature $\overline{T}$ between the hot side and cold sides of the TEC [20, 21]:

$$\overline{T} = \frac{T_{\mathrm{c}} + T_{\mathrm{h}}}{2} \tag{37}$$

Generally the expression ZT is written without indicating the averaging symbol for $\overline{\mathrm{T}}$. The parameter ZT represents the efficiency of the semiconductor materials of N-type and P-type

thermoelements. In this case, a thermoelectric semiconductor with a higher figure of merit is advantageous because it gives a superior cooling power. To obtain a higher figure of merit, a thermoelectric material optimization is required. This means to optimize the ZT dimensionless parameter by a maximization of the power factor, which depends on material properties like electrical conductivity and Seebeck coefficient, as well as a minimization of the thermal conductivity [1].

The best materials with high ZT are high doped semiconductors. Metals have relatively small Seebeck coefficients, and insulators have low electrical conductivity. The thermoelectric cooling materials are alloys which contain bismuth telluride (Bi_2Te_3) with antimony telluride (Sb_2Te_3) (like p-type $Bi_{0.5}Sb_{1.5}Te_3$ composites) [22] and Bi_2Te_3 with bismuth selenide Bi_2Se_3 (like n-type $Bi_2Te_{2.7}Se_{0.3}$) [23], each having $ZT \cong 1$ at room temperature [21]. The thermoelectric materials with good electrical properties and low thermal conductivities are bulk materials and nanostructured materials considering the dimensionless figure of merit $ZT \geq 1$ [24, 25].

The figure of merit of thermoelectric modules rises with the Seebeck coefficient, while the cooling capacity of the heat sink becomes narrow [26]. Much more, the figure of merit of a thermoelectric element limits the temperature differential achieved between the sides of the module, while the length-to-surface ratio for the thermoelements defines the cooling capacity [3].

The number of thermoelements in a thermoelectric module mainly depends on the required cooling capacity and the maximum electric current [9]. An expression for the cooling capacity shows that it also depends on thermal and electrical contact resistances (at both sides of the thermoelectric module), as well as the thermoelement length of the module [20]:

$$\dot{Q}_c = \frac{k \cdot (\Delta T_{\max} - \Delta T)}{l + 2 \cdot r \cdot l_c + r \cdot l_c \cdot COP^{-1}} \tag{38}$$

where l_c is the thickness of the contact layers, r is the thermal contact parameter (which is the ratio between the thermal conductivity of the thermoelements and the thermal conductivity of the contact layers), COP is the coefficient of performance and $\Delta T_{\max}$ the maximum temperature difference.

An insignificant effect of the contact resistances on the cooling capacity is observed for the thermoelements with long lengths, while significant changes of the cooling capacity are obtained when the contact resistances are improved, and this is for the case of short thermoelements [27]. The maximum cooling capacity $\dot{Q}_{c_{max}}$ and the maximum $COP_{\max}$ are used in design to find the operating conditions [28]. The maximum temperature difference $\Delta T_{\max}$ obtainable between the hot and cold sides always occurs at $I_{\max}$, $V_{\max}$ and $\dot{Q}_c = 0$:

$$\Delta T_{\max} = \left(T_h + \frac{1}{Z}\right) - \left[\left(T_h + \frac{1}{Z}\right)^2 - T_h^2\right]^{\frac{1}{2}} \tag{39}$$

The maximum current represents the current which gives the maximum possible temperature difference $\Delta T_{\max}$ which takes place when $\dot{Q}_c = 0$ [4]. Practically, operating under the maximum

current, there is insufficient current to obtain $\Delta T_{\max}$. Working above the maximum current, the power dissipation inside the TEC starts to rise the device temperature and to decrease ΔT. The maximum current is almost constant which is the operating range of the device:

$$I_{\max} = \alpha_{NP} \cdot (T_h - \Delta T_{max}) \cdot R^{-1} \tag{40}$$

The maximum cooling capacity $\dot{Q}_{c_{\max}}$ for a TEC is the maximum thermal load obtained when $\Delta T = 0$ and $I = I_{\max}$:

$$\dot{Q}_{c_{max}} = \alpha_{NP}{}^2 \left(T_h^2 - \Delta T_{\max}^2\right) \cdot (2R)^{-1} \tag{41}$$

The maximum voltage represents the DC voltage which gives $\Delta T_{\max}$ at $I = I_{\max}$. In this case *COP* has a minimum value. At maximum voltage the power dissipation inside the TEC starts to rise the device temperature and to decrease ΔT. The maximum voltage depends on the temperature:

$$V_{\max} = \alpha_{NP} \cdot T_h \tag{42}$$

The coefficient of performance (*COP*) represents the heat absorbed at the cold junction or cooling capacity, divided by the input electrical power:

$$COP = \frac{\dot{Q}_c}{P_{el}} \tag{43}$$

Various papers explain the *COP* dependence of the characteristics of the materials on the Thomson effect and on temperature. The TEC performance is improved by raising the figure of merit of the thermoelectric elements and considering the Thomson effect [29]. The validity of the Thomson effect is taken into account in the relationships of the cooling capacity and input electrical power and implicitly in the *COP* relationship, if the dependence on temperature of Seebeck coefficient is considered [30]. In this case the Thomson effect gives a reduction with about 7.1% for the input electrical power and with about 7% for the cooling capacity considering the positive values of the Thomson coefficient; instead, an improvement in both the input electrical power and the cooling capacity is observed for negative values of the Thomson coefficient [31].

The *COP* is also influenced by the thermal and electrical contact resistances. The *COP* of the thermoelectric module can be improved up to 60% by decreasing the electrical contact resistances [27]. Furthermore, the *COP* depends on the thermoelement length. The *COP* rises with the increment of the thermoelement length. For a thermoelement with a shorter length, the contact resistance becomes closer to the resistance of the thermoelement, notably affecting this indicator [27].

The maximum *COP* (indicated as $COP_{\max}$) of a TEC is used for its sizing [9, 20]. The $COP_{\max}$ has the benefit of minimum input electrical power, therefore, minimum total heat to be rejected by the heat sink: $\dot{Q}_h = \dot{Q}_c + P_{el}$.

The $COP_{\max}$ depends on the current and does not depend on the number of TEC pairs [32, 27]:

$$COP_{\max} = \left(R{\cdot}I^2 + \alpha_{\mathrm{NP}}{\cdot}I{\cdot}\Delta T\right)^{-1}{\cdot}\left(\alpha_{\mathrm{NP}}{\cdot}I{\cdot}T_{\mathrm{c}} - k{\cdot}\Delta T - \frac{R{\cdot}I^2}{2}\right) \tag{44}$$

The $COP_{\max}$ and the maximum temperature difference $\Delta T_{\max}$ are affected by the figure of merit. The $COP_{\max}$ is reached at low T_{h}, high T_{c} and high Z [33]:

$$COP_{max} = \underbrace{T_c{\cdot}\Delta T^{-1}}_{COP_C}{\cdot}\underbrace{\left(\sqrt{1+ZT} - T_h{\cdot}{T_c}^{-1}\right){\cdot}\left(\sqrt{1+ZT}+1\right)^{-1}}_{COP_r} \tag{45}$$

where COP_C is the (ideal) Carnot COP and COP_r is the relative COP. The COP depends on the temperature difference. Mainly, the COP rises with the reduction of the temperature difference ΔT. For household applications, to obtain an adequate cooling effect, the temperature differential between the sides of TEC is considered to be about $\Delta T = 25 \div 30$ K. In this case, the values $COP = 0.5 \div 0.7$ represent about 50% of the COP of a vapour compressor refrigerator [34].

3. Methods to enhance the TEC performance in refrigeration units

Some methods to enhance the TEC performance are [35]:

- Development of thermoelectric materials with high performance
- TEC design
- Thermal design
- Optimization of the internal temperature controller of the insulated compartment

3.1. Development of thermoelectric materials with high performance

A thermoelectric refrigerator unit operates with COP typically less 0.5 due to the limited cooling temperature to $\Delta T_{\max} \cong 20$ K under the ambient temperature [20]. **Figure 6** shows a comparison of the theoretical COP of a TEC with respect to household refrigerators [36]. Refrigerators with thermoelectric modules with materials based on alloys of Bi_2Te_3 have a COP about 1 [9] which is low enough to be competitive to the vapour-compression systems with $COP = 2 \div 4$ [37–39]. The low COP values of TECs are not considered a drawback. These systems are more suitable for a niche market sector (below 25 W) such as military and medical industries, in applications such as temperature stabilization of semiconductor lasers and vaccine cooling. Furthermore, they are also suitable for the civil market (e.g., portable refrigeration, car-seat cooler, high-quality beverage conservators). For these applications, the thermoelectric elements have the advantages that do not suffer vibrations and shocks [21, 40–42].

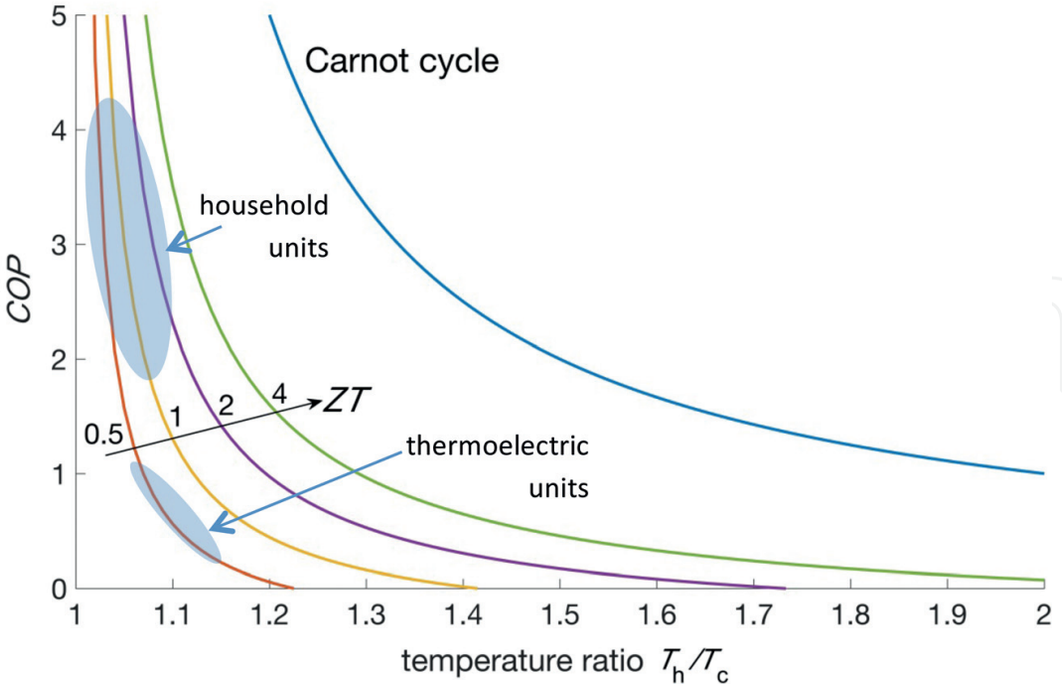

Figure 6. Chart of *COP* vs. temperature ratio for different refrigerators.

3.2. TEC design

TEC design involves the choice of number of thermocouples and thermoelement length and is carried out by looking at the module parameters. For example, for domestic refrigeration the thermoelement length optimization is strongly linked to *COP*, cooling capacity and material consumption. To improve *COP* and cooling capacity, the contact resistances, especially thermal contact resistance, must be reduced.

In devices with long thermoelements, the *COP* is high, and the contact resistances have a little effect on the cooling capacity, while in devices with short thermoelements, the contact resistances have an increased influence on the cooling capacity; in particular, starting from a long thermoelement and reducing its length, the cooling capacity increases up to a maximum value; then it decreases sharply [20].

As mentioned above, the thermal performance of a TEC depends on the thermoelectric material properties which change with the TEC operating temperature. Some manufacturers use the maximum design parameters and the performance chart [43]. The performance chart takes ΔT and $\dot{Q}_c$ as inputs and determines the current and thus the voltage needed to produce the cooling effect. Another possibility is to consider voltage, current and ΔT as known quantities (e.g. measured) in order to find $\dot{Q}_c$. A key aspect of the use of the TEC performance chart is that the module parameters are considered to be known and unchanged for different devices, while actually these parameters change because of the outcomes of the manufacturing process. The design procedure illustrated in [43] is simplified by considering the thermal resistance of the heat sink as one of the key parameters, avoiding the heat transfer analysis of the heat sink.

3.3. Thermal design

Thermal design involves the determination of the heat sink geometry considering the thermal resistances and the optimization of the heat sink characteristic.

The heat sink located on the hot side is useful to dissipate heat from the TEC system to the environment and is considered an important factor affecting the TEC performance. Therefore, to enhance the TEC performance, the heat sink must have a low thermal resistance (to be minimized). Important TEC efficiency improvements are obtained by optimization of the different types of heat exchangers at the hot side (water-air system with a cold plate, pump and fan coil, finned heat sink with fan, heat pipe with fan) [44].

A normal heat sink uses fins to increase heat transfer surface. When the thermal resistance of the heat sink is computed, it is necessary to take into account an additional heat thermal resistance of the thermal grease applied to provide a good thermal contact between TEC and heat sink [45]. The design of the heat sinks is presented in [4], where some aspects useful to find the optimal heat sink geometry (fin thickness and position) are detailed.

Sometimes at the hot side of TEC, thermal storage using phase change materials (PCMs) or a heat pipe heat exchanger may take the place of a heat sink with fins in order to reduce the temperature T_c of the TEC.

For *thermal storage*, the heat sink is designed to have a high storage capacity to keep the sink temperature less than the junction temperature. In this case, PCMs are useful to improve the performance of the thermoelectric refrigerator. These high-energy-density materials have the advantage that the heat is transferred at constant temperature. In this case, T_c is constant during the phase change, so that $\dot{Q}_c$ and *COP* remain constant as well. For a conventional refrigerator, the utilization of a heat sink with fins at the cold side of the TEC supposes a fast T_c reduction until ΔT_{max} of the cooler is obtained, while using PCMs a slow reduction of the cold side temperature till ΔT_{max} is obtained. Furthermore, PCMs operate in a wide range of phase change temperatures, providing different alternatives to be used at the hot side and at the cold side of the TEC [46]. These materials are very suitable for different types of thermoelectric refrigerators for food (domestic refrigerators; refrigerators/freezers; hotel room minibar refrigerators preferred for their silent operation; refrigerators for mobile homes, trucks, recreational vehicles, and cars; food service refrigerators for airborne application; and portable picnic coolers) as well as for medicine storage which need precise temperature control [8, 46]. Refrigerators based on PCMs exhibit useful storage capacity behaviour in case of blackout, as they are able to limit the temperature variation during a blackout much more than other materials.

The *heat pipes* are heat exchangers with very high thermal conductivity using ethanol or methanol as refrigerant water. They are used on the both sides of the TEC to dissipate both the cooling and waste heat to the heat sinks. If heat pipes with a thermosiphon are used at the hot side of the TEC, the waste heat is rejected to the environment by natural or forced convection. These systems have a low thermal resistance, leading to reduction of the temperature differential between the hot side temperature of the TEC and the environmental temperature. The heat pipes are used at the cold side of TEC to keep T_c constant during peak and

off-electricity times [46, 47]. Two prototypes of thermoelectric refrigerator are described in [48], one with finned heat sink and the other one with a finned heat sink integrated in an aluminum thermosiphon in which phase change occurs. The thermosiphon depends on the specific latent heat at the phase change from vapour state to liquid state, useful to disperse the heat efficiently to the environment. The results of the experimental heat sink optimization demonstrated that the thermal resistance between the hot side of the TEC and the environment reduced with about 23.8% at 293 K environment temperature and 51.4% at 308 K, with respect to a commercial finned heat sink, and between 13.8% and 45% with respect to an optimized finned heat sink. Much more, the *COP* of this prototype is 26% at ambient temperature of 293 K, achieving 36.5% improvement at 303 K.

3.4. Optimization of the internal temperature controller of the insulated compartment

The operating conditions of a thermoelectric refrigerator depend on parameters as environment temperature, humidity, lower setpoint of the internal temperature and difference between higher and lower setpoints of the internal temperature [49].

In vapour-compression refrigerators, the internal temperature control inside the insulated compartment is generally inaccurate due to the multitude of start and stop cycles made by the compressor, leading to a temperature variation bigger than 8°C, with a negative effect on the quality of the food and on the conservation of the perishable food [50, 51]. This represents a drawback for these refrigerators compared with the thermoelectric refrigerators in which there are no start and stop cycles and the supply voltage gradually increases. However, overall the thermoelectric refrigerators are not competitive with vapour-compression refrigerators in terms of *COP* [10, 11, 48].

Most of the thermoelectric refrigerators have on/off control systems for the internal temperature. This control is critical in the period in which the TEC is switched off, because in this period, the heat stored in the heat sink connected to the hot terminal returns into the refrigerator compartment; in this way, the power consumption of the refrigerator increases and the *COP* decreases [11].

Vian and Astrain [50] carried out a study of the total power consumption on a hybrid thermoelectric system (with vapour freezer and refrigerator compartments and a thermoelectric compartment) at ambient temperature of 25°C. To optimize the system, a thermal bridge (aluminium slab) was used between the freezer compartment and the thermoelectric compartment. This thermal bridge was useful to transfer the heat flow rate from the thermoelectric compartment to the freezer in order to maintain a constant temperature of 0°C inside the thermoelectric compartment. The power consumption in these environmental conditions for each compartment was 0.67 kWh/day for the refrigerator, 0.58 kWh/day for the freezer and 0.2 kWh/day for the thermoelectric system. The results demonstrated that the total electric power consumption reduced from 63.3 W to 49.9 W (20% improvement) due to the thermal bridge. If the environmental conditions are modified (e.g., a rise of the temperature at 30°C), the total power consumption for this unit rises by 30%. Further studies showed that the thermoelectric refrigerator works in any operating condition, but the utilization of on/off

http://dx.doi.org/10.5772/intechopen.75439

control systems at a maximum voltage decreases the electric power consumption about 40% and raises the *COP* near the maximum value obtained with the control system [11]. In addition, in [49] a reduction of electric power consumption was obtained by experimental optimization of the temperature controller for a thermoelectric refrigerator in stationary state. Their work experimentally demonstrated that the on/off temperature control system used in commercial thermoelectric refrigerators is not so efficient, but is used due to its simplicity and low cost. More efficient temperature control systems applied by the manufacturers to increase the performance of the thermoelectric refrigerator include the use of different voltage supply levels for the modules or the exploitation of proportional-integral-differential control systems. However, these control systems have a higher cost with respect to the on/off control system [11]. A more elaborated idling voltage control system was proposed from experimental optimization in [49], obtaining a 32% reduction of the electric power consumption and a *COP* growth of 64% compared with the normal on/off temperature control system. In this way, in the long term, the savings due to lower consumption compensate for the higher cost of the idling voltage control system with respect to the cost of the on/off control system.

4. Thermoelectric refrigeration unit applications

In spite of their relatively low efficiency with respect to other refrigeration technologies, the TEC technologies are experiencing a period of development, with subsequent efficiency improvement and reduction of the manufacturing costs [52]. One of the drivers that have increased the interest in the development and use of TECs as refrigerators is the absence of environmental pollution in the TEC operation, in particular, the absence of chlorofluorocarbon (CFC) issues. The current trends towards replacement of CFCs consider good solutions with low global warming potential (GWP) using natural refrigerants like CO_2 used at pressures much higher than traditional refrigerants [6, 53]. Further drivers to increase the TEC applications depend on positive aspects of the TECs such as low noise, possibility of operation in different positions, absence of mechanical vibrations, ease of transportation and possibility to obtain accurate temperature control.

Today, thermoelectric refrigerators are the most significant applications at the commercial level [17, 40]. In addition to domestic refrigerators [10, 54, 60], other applications have been developed for food-related services, such as portable refrigerators [55–57], food expositors, refrigerators mounted on vehicles for perishable food transportation as well as low-power refrigerators for minibar, hotel room, offices, boats and aircraft services [8]. Further applications are available for the medical sector (vaccine transportation and instruments for blood coagulators, dew point sensors and others), for the military sector and for scientific devices subject to precise temperature control [58]. In addition, thermoelectric systems are found in the automobile industry for air conditioning or car-seat coolers [59] and in different applications to the microelectronics sector [60, 61].

Besides the applications mentioned above, the present trend towards the use of green energy raises the attention on the possibility of supplying the thermoelectric refrigerator through

energy produced from renewable sources. The refrigerators powered by renewable sources may work in stand-alone of off-grid connection. To connect a thermoelectric refrigerator to the PV module in off-grid mode, the possibilities are [8]:

- the refrigerator is directly powered by the PV panel (the main components are the PV panel, the battery bank, the battery charge controller and the refrigerator); and
- the refrigerator is indirectly powered by the PV panel (the main components are the PV panel, the battery bank, the inverter for AC grid connection and the AC-supplied refrigerator).

Solar-driven thermoelectric refrigerators are of two types, namely, PV-battery thermoelectric systems and PV-PCM thermoelectric systems. The performance of the PV-battery thermoelectric systems depends on the intensity of solar radiation and temperature difference at the hot and cold sides of the TEC. In the case of PV-PCM thermoelectric systems, the PV is directly connected to the TECs having PCMs fixed at the cold side to replace the battery. Thermal storages have generally restricted capacity, and to improve this in some applications, the thermoelectric units use PCM integrated with thermal diodes [62].

Table 1 presents the technical characteristics of some selected thermoelectric refrigeration units with data available from the literature. The selected cases represent various applications with

Ref.	Volume (litres)	ΔT (°C)	Voltage (V)	Cooling capacity (W)	Electrical power input (W)	*COP*	Heat sink at the hot side	Power supply	Applications
[63]	3.6	40	18 (DC)	1.44	12	0.12	With fan	PV	Medicine storage
[64]	40	11.6	110 (AC)	25	13.75	0.69	With fan	Grid	On-grid applications
[55, 56]	—	20	13 (DC)	12	52	0.23	Finned	PV	Cold storage of vaccine, foodstuffs and drinks in remote areas, and outdoor off-grid applications
[10]	115/115/40	10	(DC)	15.6	52	0.3	With fans	Grid	Domestic refrigerator
[57]	13	22	12÷24 (DC)	15.3	95.6	0.16	With fan	PV	Off-grid areas
[65]	225	18.9	12 (DC)	11	48.1	0.23	Thermosiphon with two phase	Grid	Camping vehicles, buses, and special transports for electro medicine
[66]	21.9	40.5 /48.5/ 54.2	8/8/10.3 /11.56	5.2/6.5/ 8.8	20/30.9/40	0.26/0.21/ 0.22	Finned with fan	Grid	Laboratory
[67]	0.83	17.6	18	1.5	15.4	0.1	Finned with fan	DC	Vaccine carrier

Table 1. Technical characteristics and performance of thermoelectric refrigeration units.

different capacities (from a few litres for medicine transportation to some hundreds of litres for food storage), temperature difference, type of heat sink, AC or DC voltage input, powering from electrical grid connection or PV and electrical power input. The performance of these units is indicated with cooling capacity and *COP*.

5. Conclusions

Thermoelectric refrigeration solutions are gaining relevance because of a number of positive aspects, such as long duration, noiseless operation, limited maintenance needs, absence of flammable or toxic refrigerants, possibility of being used in different positions and in movable solutions as well as flexibility of usage through optimized control. This chapter has summarized the principles of thermoelectric refrigeration, by presenting the analytical formulations determining the heat flow rate, cooling capacity and *COP* of a TEC, illustrating the methods to enhance the TEC performance and indicating the current applications of thermoelectric refrigeration. The future improvement of the TEC performance, together with the operational flexibility of the TEC driven by appropriate control systems, will increase the variety of the applications of thermoelectric refrigeration in different contexts, from single units to their inclusion into integrated energy systems.

Author details

Diana Enescu

Address all correspondence to: diana.enescu@valahia.ro

Department of Electronics, Telecommunications and Energy, Valahia University of Targoviste, Targoviste, Romania

References

[1] Zheng JC. Recent advances on thermoelectric materials. Frontiers of Physics in China. 2008;**3**(3):269-279. DOI: 10.1007/s11467-008-0028-9

[2] Sandoz-Rosado EJ. Investigation and Development of Advanced Models of Thermoelectric Generators for Power Generation Applications [thesis]. Rochester Institute of Technology, Rochester NY, USA; 2009. 82 p. Available from: http://scholarworks.rit.edu/theses

[3] Rowe DM. Handbook of Thermoelectrics. Introduction. Boca Raton, FL: CRC Press; 1995 720 p. ISBN: 9780849301469

[4] Lee HS. Thermal Design, Heat Sinks, Thermoelectrics, Heat Pipes, Compact Heat Exchangers, and Solar Cells. NJ: Wiley; 2010. 650 p. DOI: 10.1002/9780470949979

[5] Tritt TM, Subramanian MA. Thermoelectric materials, phenomena, and applications: A Bird's eye view. MRS Bulletin. 2006;**31**:188-198. DOI: org/10.1557/mrs2006.44

[6] Tassou SA, Lewis JS, Ge YT, Hadawey A, Chaer I. A review of emerging technologies for food refrigeration applications. Applied Thermal Engineering. 2010;**30**(4):263-276. DOI: 10.1016/j.applthermaleng.2009.09.001

[7] Riffat SB, Ma X. Thermoelectrics: A review of present and potential applications. Applied Thermal Engineering. 2003;**23**(8):913-935. DOI: 10.1016/S1359-4311(03)00012-7

[8] Enescu D, Ciocia A, Mazza A, Russo A. Solutions based on thermoelectric refrigerators in humanitarian contexts. Sustainable Energy Technologies and Assessments. 2017;**22**:134-149. DOI: 10.1016/j.seta.2017.02.016

[9] Goldsmid HJ. Introduction to Thermoelectricity. Berlin Heidelberg: Springer-Verlag. Springer Series in Material Science. 2010;**121**:242. DOI: 10.1007/978-3-642-00716-3

[10] Min G, Rowe GM. Experimental evaluation of prototype thermoelectric domestic-refrigerator. Applied Energy. 2006;**83**(2):133-152. DOI: 10.1016/j.apenergy.2005.01.002

[11] Astrain D, Martínez A, Gorraiz J, Rodríguez A, Pérez G. Computational study on temperature control Systems for Thermoelectric Refrigerators. Journal of Electronic Materials. 2012;**41**(6):1081-1090. DOI: 10.1007/s11664-012-2002-0

[12] Barbieri J, Colombo E, Ndam Mungwe J, Riva F, Berizzi A, Bovo C, et al. Set 4 food project. Sustainable Energy Technologies for food utilization. 2014. Available from: www.set4food.org [Accessed: December 27, 2017]

[13] Martínez A, Astrain D, Rodríguez A, Aranguren P. Advanced computational model for Peltier effect based refrigerators. Applied Thermal Engineering. 2016;**95**:339-347. DOI: 10.1016/j.applthermaleng.2015.11.021

[14] Lee HS. Thermoelectrics: Design and materials. Western Michigan University, USA: Wiley; 2017. 887p. DOI: 10.1016/j.applthermaleng.2015.11.021

[15] Landau LD, Lifshitz EM, Pitaevskii LP. Electrodynamics of continuous media. 2nd ed. UK: Pergamon Press; 1984. 460 p. ISBN: 9788181477934

[16] Lee HS. The Thomson effect and the ideal equation on thermoelectric coolers. Energy. 2013;**56**:61-69. DOI: 10.1016/j.energy.2013.04.049

[17] Martinez A, Astrain D, Rodriguez A, Aranguren P. Advanced computational model for Peltier effect based refrigerators. Applied Thermal Engineering. 2016;**95**:339-347. DOI: 10.1016/j.applthermaleng.2015.11.021

[18] Martínez A, Astrain D, Rodríguez A. Dynamic model for simulation of thermoelectric self cooling applications. Energy. 2013;**55**:1114-1126. DOI: 10.1016/j.energy.2013.03.093

[19] Parrot JE, Penn AW. The design theory of thermoelectric cooling elements and units. Solid-State Electronics. 1961;**3**:91-99. DOI: 10.1016/0038-1101(61)90062-4

[20] Min G, Rowe DM. Improved model for calculating the coefficient of performance of a Peltier module. Energy Conversion and Management. 2000;**2**(41):163-171. DOI: 10.1016/S0196-8904(99)00102-8

[21] Chen G, Dresselhaus MS, Dresselhaus G, Fleurial JP, Caillat T. Recent developments in thermoelectric materials. International Materials Reviews. 2003;**48**(1):45-66. DOI: 10.1179/095066003225010182

[22] Suh D, Lee S, Hyeona Mun H, Park SH, Lee KH, Kim SW, Choi JY, Baik S. Enhanced thermoelectric performance of Bi0.5Sb1.5Te3-expanded graphene composites by simultaneous modulation of electronic and thermal carrier transport. Nano Energy. 2015;**13**:67-76. DOI: 10.1016/j.nanoen.2015.02.001

[23] Peng QZ, Ye Ko San YK, Samuel Khong S, Jonathan Sim J, Ezhilvalavan S, Ma J, Hoon HH. Advanced Structural and Functional Materials for Protection. In: Proceedings of the International Conference on Materials for Advanced Technologies (ICMAT2011), Symposium W; DOI: 10.4028/www.scientific.net/SSP.185

[24] Nolas GS, Poon J, Kanatzidis M. Recent developments in bulk thermoelectric materials. MRS Bulletin. 2006;**31**(3):199-205. DOI: 10.1557/mrs2006.45

[25] Biswas K, He J, Zhang Q, Wang G, Uher C, Dravid VP, Kanatzidis MG. Strained endotaxial nanostructures with high thermoelectric figure of merit. Nature Chemistry. 2011;**3**:160-166. DOI: 10.1038/nchem.955

[26] Gupta MP, Sayer M, Mukhopadhyay S, Kumar S. Ultrathin thermoelectric devices for on-chip Peltier cooling. IEEE Transactions on Computer, Packaging, and Manufacturing Technology. 2011;**1**(9):1395-1405. DOI: 10.1109/TCPMT.2011.2159304

[27] Rowe DM. Thermoelectrics Handbook: Macro to Nano. Boca Raton, FL: CRC Press Taylor & Francis; 2006 1014 p. ISBN 9780849322648

[28] Elarusi A, Attar A, Lee H. Optimal Design of a Thermoelectric Cooling/heating system for Car seat climate control (CSCC). Journal of Electronic Materials. 2017;**46**(4):1984-1995. DOI: 0.1007/s11664-016-5043-y

[29] Huang MJ, Chou PK, Lin MC. Thermal and thermal stress analysis of a thin-film thermoelectric cooler under the influence of the Thomson effect. Sensors and Actuators A-Physical. 2006;**126**(1):122-128. DOI: 10.1016/j.sna.2005.10.006

[30] Fraisse G, Ramousse J, Sgorlon D, Goupil C. Comparison of different modeling approaches for thermoelectric elements. In Energy Conversion and Management. 2013; **65**:351-356. DOI: 10.1016/j.enconman.2012.08.022

[31] Chen J, Yan Z. The influence of Thomson effect on the maximum power output and maximum efficiency of a thermoelectric generator. Journal of Applied Physics. 1996;**79**: 8823-8828. DOI: 10.1063/1.362507

[32] Chen WH, Liao CY, Hung CI. A numerical study on the performance of miniature thermoelectric cooler affected by Thomson effect. Applied Energy. 2012;**89**:464-473. DOI: 10.1016/j.apenergy.2011.08.022

[33] Bansal P, Vineyard E, Abdelaziz O. Status of not-in-kind refrigeration technologies for household space conditioning, water heating and food refrigeration. International Journal of Sustainable Built Environment. 2012;**1**:85-101. DOI: 10.1016/j.ijsbe.2012.07.003

[34] Zhang HY. A general approach in evaluating and optimizing thermoelectric coolers. Int. Journal of Refrigeration. 2010;**33**(6):1187-1196. DOI: 10.1016/j.ijrefrig.2010.04.007

[35] Gökçek M, Şahin F. Experimental performance investigation of minichannel water cooled-thermoelectric refrigerator. Case Studies in Thermal Engineering. 2017;**10**:54-62. DOI: 10.1016/j.csite.2017.03.004

[36] Chen G, Shakouri A. Heat transfer in nanostructures for solid-state energy conversion. Journal of Heat Transfer. 2001;**124**(2):242-252. DOI: 10.1115/1.1448331

[37] Gauger DC, Shapiro HN, Pate MB. Alternative technologies for refrigeration and air-conditioning applications. United States Environmental Protection Agency. Project Summary EPA/600/SR-95/066; 1995

[38] Bell L. Use of thermal isolation to improve thermoelectric system operating efficiency. In: Proceeding 21st Int. Conf. on Thermoelectrics, ICT'02; 29–29 Aug. 2002; Long Beach, California (USA), p. 477-487. DOI: 10.1109/ICT.2002.1190363

[39] Hermes CJL, Barbosa Jr JR. Thermodynamic comparison of Peltier, Stirling, and vapor compression. Applied Energy. 2012;**91**:51-58. DOI: 10.1016/j.apenergy.2011.08.043

[40] Zhao D, Tan G. A review of thermoelectric cooling: Materials, modeling and applications. Applied Thermal Engineering. 2014;**66**:15-24. DOI: 10.1016/j.applthermaleng.2014.01.074

[41] Enescu D, Virjoghe EO. A review on thermoelectric cooling parameters and performance. Renewable & Sustainable Energy Reviews. 2014;**38**:903-916. DOI: 10.1016/j.rser.2014.07.045

[42] Yeom J, Shannon MA, Singh T. Micro-coolers. In: Reference Module in Materials Science and Materials Engineering. Elsevier; 2017. pp. 2-46. DOI: 10.1016/B978-0-12-803581-8.00568-3

[43] Huang BJ, Chin CJ, Duang CL. A design method of thermoelectric cooler. International Journal of Refrigeration. 2000;**23**:208-218. DOI: 10.1016/S0140-7007(99)00046-8

[44] Astrain D, Aranguren P, Martínez A, Rodríguez A, Pérez MG. A comparative study of different heat exchange systems in a thermoelectric refrigerator and their influence on the efficiency. Applied Thermal Engineering. 2016;**103**:1289-1298. DOI: 10.1016/j.applthermaleng.2016.04.132

[45] Ritzer TM, Lau PG. Economic Optimization of Heat Sink Design. In: Proceedings of the 13th Int. Conference on Thermoelectrics; 30 August-1September; Kansas City, Missouri (USA); 1995; AIP Conference Proceedings 316, 177 (1994). DOI: 10.1063/1.46788

[46] Riffat SB, Omer SA, Ma X. A novel thermoelectric refrigeration system employing heat pipes and a phase change material: An experimental investigation. Renewable Energy. 2001;**23**(2):313-323. DOI: 10.1016/S0960-1481(00)00170-1

[47] Faghri A. Heat Pipe Science and Technology. Taylor & Francis; 1995 859 p. ISBN 978-1560323839

[48] Astrain A, Vián JG, Domínguez M. Increase of COP in the thermoelectric refrigeration by the optimization of heat dissipation. Applied Thermal Engineering. 2003;**23**(17):2183-2200. DOI: 10.1016/S1359-4311(03)00202-3

[49] Martinez A, Astrain D, Rodríguez A, Pérez MG. Reduction in the electric power consumption of a thermoelectric refrigerator by experimental optimization of the temperature controller. Journal of Electronic Materials. 2013;**42**(7):1499-1503. DOI: 10.1007/s11664-012-2298-9

[50] Vián JG, Astrain DD. Development of a hybrid refrigerator combining thermoelectric and vapor compression technologies. Applied Thermal Engineering. 2009;**29**(16):3319-3327. DOI: 10.1016/j.applthermaleng.2009.05.006

[51] He MG, Li TC, Liu ZG, Zhang Y. Testing of the mixing refrigerants HFC152a/HFC125 in domestic refrigerator. Applied Thermal Engineering. 2005;**25**(8–9):1169-1181. DOI: 10.1016/j.applthermaleng.2004.06.003

[52] Sarbu I, Sebarchievici C. Review of solar refrigeration and cooling systems. Energy and Buildings. 2013;**67**:286-297. DOI: 10.1016/j.enbuild.2013.08.022

[53] Aprea C, Greco A, Maiorino A. An experimental evaluation of the greenhouse effect in the substitution of R134a with CO_2. Energy. 2012;**45**:753-761. DOI: 10.1016/j.energy.2012.07.015

[54] Rodríguez A, Vián JG, Astrain D. Development and experimental validation of a computational model in order to simulate ice cube production in a thermoelectric ice-maker. Applied Thermal Engineering. 2009;**29**:2961-2969. DOI: 10.1016/j.applthermaleng.2009.03.005

[55] Dai YJ, Wang RZ, Ni L. Experimental investigation on a thermoelectric refrigerator driven by solar cells. Renewable Energy. 2003;**28**:949-959. DOI: 10.1016/S0960-1481(02)00055-1

[56] Dai Y, Wang J, Ni L. Experimental investigation and analysis on a thermoelectric refrigerator driven by solar cells. Journal of Solar Energy Materials & Solar Cells. 2003;**77**(4): 377-391. DOI: 10.1016/S0927-0248(02)00357-4

[57] Abdul-Wahab SA, Elkamel A, Al-Damkhi AM, Al-Habsi IA, Al-Rubaiey HS, Al-Battashi AK, Ali R, Al-Tamimi AR, Al-Mamari KH, Chutani MU. Design and experimental investigation of portable solar thermoelectric refrigerator. Renewable Energy. 2009;**34**:30-34. DOI: 10.1016/j.renene.2008.04.026

[58] Marlow R, Burke E. Module design and fabrication. In: Rowe DM, editor. Handbook of Thermoelectrics: Introduction. Boca Raton, FL: CRC Press; 1995. p. 591. ISBN 9780849301469

[59] Choi HS, Yun S. Whang K-il. Development of a temperature-controlled car-seat system utilizing thermoelectric device. Applied Thermal Engineering. 2007;**27**(17–18):2841-2849. DOI: 10.1016/j.applthermaleng.2006.09.004

[60] Gordon JM, Ng KC, Chua HT, Chakraborty A. The electro-adsorption chiller: A miniaturized cooling cycle with applications to micro-electronics. International Journal of Refrigeration. 2002;2**5**(8):1025-1033

[61] Zhang Y, Christofferson J, Shakouri A, Zeng G, Bowers JE, Croke E. On-Chip high speed localized cooling using Superlattice Microrefrigerators. IEEE Transactions on Components and Packaging Technologies. 2006;**29**(2):395-401

[62] Aste N, Del Pero C, Leonforte F. Active refrigeration technologies for food preservation in humanitarian context-a review. Sustainable Energy Technologies and Assessments. 2017; **22**:150-160. DOI: 10.1016/j.seta.2017.02.014

[63] Field RL. Photovoltaic/thermoelectric refrigerator for medicine storage for developing countries. Solar Energy. 1980;**25**:445-447. DOI: 10.1016/0038-092X(80)90452-1

[64] Bansal PK, Martin A. Comparative study of vapour compression, thermoelectric and absorption refrigerators. International Journal of Energy Research. 2000;**24**(2):93-107. DOI: 10.1002/(SICI)1099-114X(200002)24:2<93::AID-ER563>3.0.CO;2-6

[65] Vián JG, Astrain D. Development of a thermoelectric refrigerator with two phase thermosyphons and capillary lift. Applied Thermal Engineering. 2009a;**29**:1935-1940. DOI: 10.1016/j.applthermaleng.2008.09.018

[66] Jugsujinda S, Vora-ud A, Seetawan T. Analyzing of thermoelectric refrigerator performance. Procedia Engineering. 2011;**8**:154-159. DOI: 10.1016/j.proeng.2011.03.028

[67] Ohara B, Sitar R, Soares J, Novisoff P, Nunez-Perez A, Lee H. Optimization strategies for a portable thermoelectric vaccine refrigeration system in developing communities. Journal of Electronic Materials. 2015;**44**(6):1614-1626. DOI: 10.1007/s11664-014-3491-9